

Crystal Structures and Magnetism of Binuclear Iron(III) Complexes with a Linear Oxo-bridge, $[\text{Fe}_2\text{O}(\text{bbimae})_2\text{X}_2][\text{NO}_3]_2$ {bbimae = 2-[bis(benzimidazol-2-ylmethyl)amino]ethanol, X = Cl or NCS} †

Kazuhiro Takahashi, Yuzo Nishida,* Yonezo Maeda, and Sigeo Kida

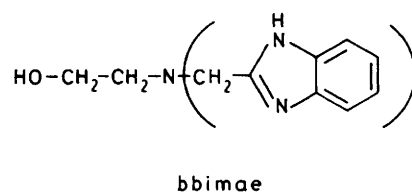
Department of Chemistry, Faculty of Science, Kyushu University 33, Hakozaki Fukuoka 812, Japan

The crystal structures of the oxo-bridged binuclear iron(III) complexes $[\text{Fe}_2\text{O}(\text{bbimae})_2\text{X}_2][\text{NO}_3]_2$ {X = Cl (1) or NCS (2); bbimae = 2-[bis(benzimidazol-2-ylmethyl)amino]ethanol} have been determined by X-ray diffraction methods. Crystals of (1) are monoclinic with $a = 11.949(3)$, $b = 15.901(4)$, $c = 11.326(2)$ Å, $\beta = 109.36(2)^\circ$, space group $P2_1/n$, and $Z = 2$. Crystals of (2) are orthorhombic with $a = 16.384(2)$, $b = 19.804(2)$, $c = 13.600(2)$ Å, space group $Pbca$, and $Z = 4$. Both crystals are composed of centrosymmetric dimeric cations with a linear Fe–O–Fe bond and nitrate counter ions. The iron–iron and iron–oxo distances are 3.563(1) and 1.7816(7) Å for (1) and 3.559(1) and 1.7795(8) Å for (2). Mössbauer spectra reveal the presence of high-spin iron(III) atoms in both complexes. The magnetic moments of 1.81(295 K) and 0.73 B.M. (98 K) for (1) and 1.82 (295 K) and 0.89 B.M. (98 K) for (2) indicate an antiferromagnetic interaction between the two iron(III) atoms. The $-J$ value was evaluated as 103 cm^{-1} for (1), which falls in the range (95–110 cm^{-1}) of previously reported oxo-bridged complexes with Fe–O–Fe bond angles in the range 139–180°.

Polynuclear iron(III) complexes bridged by oxygen donor ligands play an important role in the inorganic and bioinorganic chemistry of iron(III) ions. The simplest of these are dimeric species which contain an $[\text{Fe}_2\text{O}]^{4+}$ or $[\text{Fe}_2(\text{OH})_2]^{4+}$ skeleton.^{1–3} Since the presence of an $[\text{Fe}_2\text{O}]^{4+}$ skeleton has been indicated for oxyhemerythrin⁴ and ribonucleotide reductase,⁵ great interest has arisen in the magnetic and spectral properties of complexes of this type.

It is known that oxo-bridged iron(III) complexes display substantial antiferromagnetism due to superexchange coupling between the $S = \frac{5}{2}$ Fe^{III} ions via the oxo-bridge.⁶ A series of such dimers have been prepared, and have displayed a magnetochemistry well described by the $-2J\mathcal{S}_1 \cdot \mathcal{S}_2$ exchange Hamiltonian with $S_1 = S_2 = \frac{5}{2}$. It should be noted that their $-J$ values fall in the range 90–110 cm^{-1} , irrespective of the coordination number, the non-bridging ligands, and the Fe–O–Fe bridging angle (139–180°).^{6–9} We find this result curious since the magnitude of antiferromagnetic interaction in such systems might be expected to depend upon the overlap between metal 3d and oxygen 2p orbitals, and hence is thought to be sensitive to the Fe–O–Fe bridging angle. However, few systematic works have been reported on this subject.⁸

We have been investigating metal complexes with tripodal ligands,¹⁰ and have reported the preparation and crystal structures of metal complexes ($M^{2+} = \text{Zn, Cu, Ni, Co, Mn, or VO}$) of 2-[bis(benzimidazol-2-ylmethyl)amino]ethanol (bbimae).¹¹ Very recently Nishida *et al.*¹² have synthesized and determined the crystal structure of a di- μ -alkoxo-diron(III) complex of bbimae. In the course of the preparative studies on iron(III) complexes of bbimae, we have found that the oxo-bridged binuclear iron(III) complexes are formed when



the reaction mixture [iron(III) and bbimae in dimethyl sulphoxide–methanol] contains 20–30% of water. In this paper we report the syntheses, crystal structures, and the magnetic properties of the oxo-bridged iron(III) complexes $[\text{Fe}_2\text{O}(\text{bbimae})_2\text{X}_2][\text{NO}_3]_2$ [X = Cl (1) or NCS (2)], hopefully to elucidate the relationship between their magnetic interaction and Fe–O–Fe bond angle.

Experimental

Materials.—All chemicals employed were reagent-grade and used without further purification. The ligand bbimae was prepared by the published method.^{11b}

$[\text{Fe}_2\text{O}(\text{bbimae})_2\text{Cl}_2][\text{NO}_3]_2$ (1).—A methanol solution (10 cm^3) of $\text{Fe}(\text{NO}_3)_3 \cdot 9\text{H}_2\text{O}$ (810 mg, 2 mmol) and a dimethyl sulphoxide–methanol (1:1 v/v, 25 cm^3) solution of bbimae·H₂O (680 mg, 2 mmol) were mixed. To this solution was added an aqueous solution (15 cm^3) of KCl (220 mg, 3 mmol). The resulting solution was allowed to stand for one week. The brown rhombohedral prisms deposited were filtered off, and dried *in vacuo* over P₂O₅. (Found: C, 44.80; H, 4.00; N, 17.30. $\text{C}_{36}\text{H}_{38}\text{Cl}_2\text{Fe}_2\text{N}_{12}\text{O}_9$ requires C, 44.80; H, 4.00; N, 17.40%.)

$[\text{Fe}_2\text{O}(\text{bbimae})_2(\text{NCS})_2][\text{NO}_3]_2$ (2) was obtained as black-brown prisms by a similar method by adding NH₄NCS instead of KCl (Found: C, 45.00; H, 3.70; N, 19.10. $\text{C}_{38}\text{H}_{38}\text{Fe}_2\text{N}_{14}\text{O}_9\text{S}_2$ requires C, 45.15; H, 3.80; N, 19.40%.)

Measurements.—Magnetic susceptibilities were measured by the Faraday method over the temperature range 98–295 K. The instrument was equipped with a Kahn-2000 electrobalance and calibrated with $[\text{Ni}(\text{NH}_2\text{CH}_2\text{CH}_2\text{NH}_2)_3]\text{S}_2\text{O}_3$.¹³ Dia-

† μ -Oxo-bis[2-[bis(benzimidazol-2-ylmethyl)amino]ethanol-*NN'N''O*]chloroiron(III) dinitrate and μ -oxo-bis[2-[bis(benzimidazol-2-ylmethyl)amino]ethanol-*NN'N''O*]isothiocyanatoiron(III) dinitrate respectively.

Supplementary data available (No. SUP 56319, 9 pp.): anisotropic thermal parameters, full lists of bond lengths and angles, H-atom coordinates. See Instructions for Authors, *J. Chem. Soc., Dalton Trans.*, 1985, Issue 1, pp. xvii–xix.

Non-S.I. units employed: B.M. $\approx 9.27 \times 10^{-24}$ A m², $\chi_{\text{c.g.s.u.}} = \chi_{\text{s.i.}} \times 10^6/4\pi$.

Table 1. Crystal data for $[\text{Fe}_2\text{O}(\text{bbimae})_2\text{Cl}_2][\text{NO}_3]_2$ (1) and $[\text{Fe}_2\text{O}(\text{bbimae})_2(\text{NCS})_2][\text{NO}_3]_2$ (2)

Complex	(1)	(2)
Formula	$\text{C}_{36}\text{H}_{38}\text{Cl}_2\text{Fe}_2\text{N}_{12}\text{O}_9$	$\text{C}_{38}\text{H}_{38}\text{Fe}_2\text{N}_{14}\text{O}_9\text{S}_2$
<i>M</i>	965.4	1 010.6
Crystal system	Monoclinic	Orthorhombic
Space group	$P2_1/n$	$Pbca$
<i>a</i> /Å	11.949(3)	16.384(2)
<i>b</i> /Å	15.901(4)	19.804(2)
<i>c</i> /Å	11.326(2)	13.600(2)
β /°	109.36(2)	90
<i>U</i> /Å ³	2 030.5(9)	4 413(1)
<i>D_m</i> /g cm ⁻³ ^a	1.60	1.57
<i>D_c</i> /g cm ⁻³	1.58	1.53
<i>Z</i>	2	4
<i>F</i> (000)	992	2 080
$\mu(\text{Mo-K}\alpha)/\text{cm}^{-1}$	9.6	8.6
Crystal size/mm	0.2 × 0.4 × 0.4	0.3 × 0.3 × 0.4
No. of total reflections	3 876	5 165
No. of unique reflections		
$[F_o > 3\sigma(F_o)]$	2 713	2 167

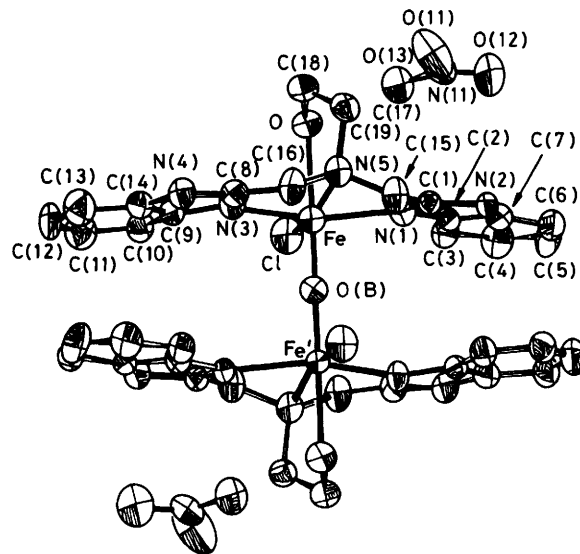
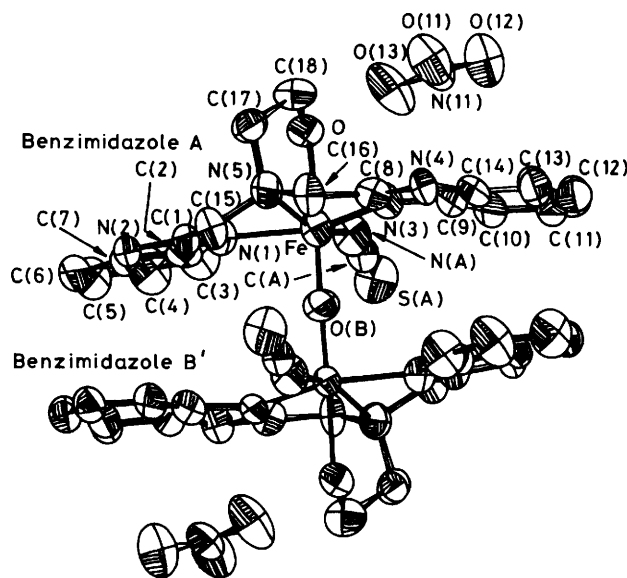
^a Measured by flotation in $n\text{-C}_6\text{H}_{14}\text{-BrCH}_2\text{CH}_2\text{Br}$.

magnetic corrections of -232×10^{-6} c.g.s.u. per Fe for (1) and -240×10^{-6} c.g.s.u. per Fe for (2) were calculated by using Pascal's constants.¹⁴ Effective magnetic moments were calculated using $\mu_{\text{eff.}} = \sqrt{7.998\chi T}$, where χ is the atomic magnetic susceptibility. Mössbauer spectra were obtained by the published method.¹⁵ Infrared spectra were obtained with a Hitachi-Perkin-Elmer model 225 spectrophotometer on KBr discs.

Collection of Diffraction Data.—Diffraction data were collected at 294 ± 1 K with a Rigaku AFC-5 automatic four-circle diffractometer using graphite-monochromated Mo- K_α radiation ($\lambda = 0.710$ 69 Å). The unit-cell parameters were determined by least-squares routines (*cf.* Table 1). Intensity data were collected by the θ — 2θ scan technique, in the 2θ range 4—50°, and with a scan rate of 6° min^{-1} . Three standard reflections were monitored every 100 reflections, and their intensities showed good stability during data collection. Intensity data were corrected for Lorentz and polarization effects, but not for absorption. Independent reflections with $|F_o| > 3\sigma|F_o|$ were used for the structure determination.

Structure Solution and Refinement.—Complex (1) crystallizes in the space group $P2_1/n$, with only two dimeric molecules present in the unit cell. Each molecule therefore has a centre of symmetry, corresponding to the special positions (0,0,0) or $(0, \frac{1}{2}, \frac{1}{2})$. Thus, the oxygen atom, which is located in the centre of the complex was taken to be (0,0,0), as shown in Table 2. The same phenomenon was also observed for (2) which crystallized in the orthorhombic space group $Pbca$.

The positions of the iron atoms were located by direct methods (MULTAN 78)¹⁶ and atomic co-ordinates of the other atoms determined by the combined use of direct methods and difference-Fourier syntheses. The final positional parameters with their estimated standard deviations are given in Table 2. Refinements with anisotropic thermal parameters for non-hydrogen atoms and isotropic ones for hydrogen atoms gave $R = (\sum ||F_o| - |F_c|| / \sum |F_o|) = 0.0368$ for (1) and 0.0451 for (2), and $R' = (\sum ||F_o| - |F_c||^2 / \sum |F_o|^2)^{1/2} = 0.0377$ for (1) and 0.0443 for (2). The final difference-Fourier maps showed no significant electron density, peaks being less than 0.33 for (1)

**Figure 1.** ORTEP drawing of $[\text{Fe}_2\text{O}(\text{bbimae})_2\text{Cl}_2][\text{NO}_3]_2$ (1) showing 50% probability ellipsoids**Figure 2.** ORTEP drawing of $[\text{Fe}_2\text{O}(\text{bbimae})_2(\text{NCS})_2][\text{NO}_3]_2$ (2) showing 50% probability ellipsoids

and $0.28 \text{ e } \text{Å}^{-3}$ for (2). Atomic scattering factors for Fe^{3+} , S, Cl, O, N, and C were taken from ref. 17 and those for H from ref. 18. All calculations were carried out on a Facom M-200 computer at the Computer Center of Kyushu University using a local version¹⁹ of the UNICS II and ORTEP computing systems.²⁰

Results and Discussion

Description of Structures.—The structures of complexes (1) and (2) are shown in Figures 1 and 2, respectively. In each molecule two six-co-ordinated iron atoms are bridged by a single oxygen atom, the Fe—O—Fe bond angle in both (1) and (2) being 180° due to the requirement of the centrosymmetry. Both iron atoms are surrounded by a distorted octahedral array of donor atoms (*cf.* Table 3); angles with idealized values of 90° range from 74.8° [N(1)—Fe—N(5)] to 105.3° [Cl—Fe—N(3)] in (1),

Table 2. Positional parameters ($\times 10^4$; H, $\times 10^3$) with estimated standard deviations in parentheses for $[\text{Fe}_2\text{O}(\text{bbimae})_2\text{Cl}_2][\text{NO}_3]_2$ (1) and $[\text{Fe}_2\text{O}(\text{bbimae})(\text{NCS})_2][\text{NO}_3]_2$ (2)

Atom	(1)			(2)		
	x	y	z	x	y	z
Fe	1 188(1)	182.5(3)	1 420(1)	337(1)	82.0(4)	1 238(1)
O(B)	0	0	0	0	0	0
Cl	815(1)	1 502(1)	2 022(1)			
N(A)				1 453(3)	468(3)	1 028(4)
C(A)				2 112(4)	549(3)	716(4)
S(A)				2 995(1)	648(1)	264(2)
N(1)	2 397(3)	437(2)	463(3)	582(3)	-953(2)	1 371(4)
N(2)	3 379(3)	-19(2)	-779(3)	113(3)	-2 005(2)	1 392(4)
C(1)	2 731(3)	-221(2)	-49(3)	-69(4)	-1 345(3)	1 447(4)
C(2)	2 838(3)	1 135(2)	9(3)	1 250(4)	-1 387(3)	1 247(5)
C(3)	2 722(4)	1 998(3)	202(4)	2 067(4)	-1 254(4)	1 115(6)
C(4)	3 274(4)	2 536(3)	-398(5)	2 581(5)	-1 804(4)	1 036(7)
C(5)	3 894(5)	2 251(3)	-1 152(4)	2 283(4)	-2 463(4)	1 065(7)
C(6)	3 997(4)	1 407(3)	-1 361(4)	1 483(4)	-2 604(3)	1 184(5)
C(7)	3 461(3)	855(2)	-767(4)	955(4)	-2 049(3)	1 273(4)
N(3)	417(3)	-651(2)	2 369(3)	-427(3)	919(2)	1 485(3)
N(4)	-129(3)	-1 946(2)	2 630(3)	-1 685(3)	1 332(2)	1 652(4)
C(8)	522(3)	-1 462(2)	2 146(4)	1 201(3)	781(2)	1 664(4)
C(9)	-390(3)	-608(2)	3 023(3)	-393(3)	1 619(3)	1 325(4)
C(10)	-874(4)	75(3)	3 451(4)	279(4)	2 036(3)	1 107(5)
C(11)	-1 653(4)	-97(3)	4 078(4)	103(4)	2 712(3)	978(5)
C(12)	-1 946(4)	-198(3)	4 299(4)	-688(4)	2 970(3)	1 079(5)
C(13)	-1 485(4)	-1 597(3)	3 866(4)	-1 346(4)	2 563(3)	1 315(5)
C(14)	-724(3)	-1 427(3)	3 207(4)	-1 180(3)	1 881(3)	1 430(4)
N(5)	2 095(3)	-1 098(2)	1 331(3)	-798(3)	-372(2)	1 992(3)
C(15)	2 337(4)	-1 093(2)	135(4)	-908(4)	-1 051(3)	1 552(5)
C(16)	1 236(4)	-1 764(2)	1 373(4)	-1 508(3)	77(3)	1 815(5)
C(17)	3 232(4)	-1 154(3)	2 391(4)	-625(4)	-442(3)	3 062(5)
C(18)	3 185(4)	-704(3)	3 537(4)	-95(4)	124(3)	3 428(4)
O	2 741(2)	136(2)	3 202(2)	616(2)	148(2)	2 812(3)
N(11)	5 223(3)	921(2)	2 740(3)	1 254(3)	1 692(3)	3 466(4)
O(11)	5 318(3)	154(2)	2 811(5)	522(3)	1 645(3)	3 637(5)
O(12)	5 791(3)	1 320(2)	2 188(3)	1 587(3)	2 239(2)	3 467(5)
O(13)	4 557(3)	1 285(2)	3 224(3)	1 641(3)	1 159(2)	3 264(4)

Table 3. Equations* of least-squares planes of the equatorial atoms of (1) and (2); deviations (\AA) of the atoms from the plane are given in parentheses

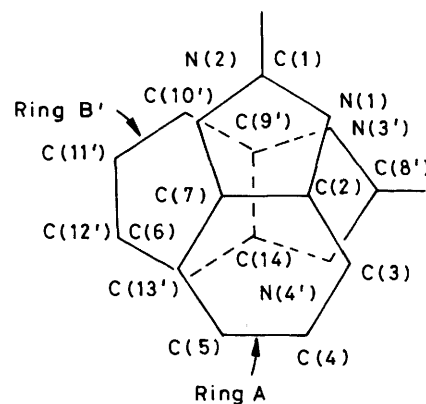
Complex (1): Plane through Cl, N(1), N(3), and N(5)
 $0.5249X + 0.0622Y + 0.6270Z = 2.0005$
 [Cl 0.095, N(1) -0.125, N(3) -0.120, N(5) 0.150, Fe -0.229, O(B) -2.000, O 2.005]

Complex (2): Plane through N(A), N(1), N(3), and N(5)
 $0.2874X + 0.0895Y + 0.9536Z = 2.0033$
 [N(A) 0.097, N(1) -0.121, N(3) -0.116, N(5) 0.139, Fe -0.224, O(B) -2.003, O 1.960]

* The equation is expressed by $AX + BY + CZ = D$, where X , Y , Z (in \AA) refer to the crystallographic axes.

and from 74.7° [N(1)-Fe-N(5)] to 105.4° [N(A)-Fe-N(3)] in (2) (cf. Table 4). A major factor in the distortion from the octahedral values may be the steric constraints of bbimae. The bond distances of Fe to N(1), N(5), O, and O(B) of (1) are longer than those of (2), as shown in Table 4.

The average Fe-N distances (cf. Table 4) in (1) and (2) are in accord with values of other high-spin iron(III) complexes. For example, in two complexes containing high-spin iron(III) atoms, $[\text{Fe}_2\text{O}(\text{O}_2\text{CCH}_3)_2(\text{Htpzb})_2]$ (Htpzb = tripyrazol-1-ylborate)²¹ and $[\text{Fe}_2\text{O}(\text{phen})_4(\text{H}_2\text{O})_2][\text{NO}_3]_4$ (phen = 1,10-phenanthroline),⁹ the mean Fe-N (2.171 and 2.168 \AA , respectively) bond lengths may be compared with the corresponding distances in (1) and (2) (2.180 and 2.168 \AA ,

**Figure 3.** Projection of atoms of benzimidazole ring A onto the plane of benzimidazole ring B' in $[\text{Fe}_2\text{O}(\text{bbimae})_2(\text{NCS})_2][\text{NO}_3]_2$ (2) (cf. Figure 2)

respectively). The iron-oxo distances in both (1) [1.7816(7) \AA] and (2) [1.7795(8) \AA] fall in the range (1.73–1.82 \AA) normally observed for binuclear iron(III) complexes with a single oxygen bridge.⁶

Intramolecular stacking between two benzimidazole rings is observed for both complexes, as illustrated in Figure 3. This stacking mode is very similar to those observed for $[\text{Cu}(\text{bbimae})\text{X}]\text{ClO}_4$ ($X = \text{Cl}$ or Br).^{11a} The planes of the two

Table 4. Selected bond distances (Å) and angles (°) with estimated standard deviations in parentheses for the co-ordination spheres of $[\text{Fe}_2\text{O}(\text{bbimae})_2\text{Cl}_2][\text{NO}_3]_2$ (1) and $[\text{Fe}_2\text{O}(\text{bbimae})_2(\text{NCS})_2][\text{NO}_3]_2$ (2)*

		(1)	(2)
Fe-X	X = Cl	2.295(1)	X = N(A) 2.003(5)
Fe-N(1)		2.113(4)	2.097(5)
Fe-N(3)		2.102(3)	2.104(4)
Fe-N(5)		2.324(3)	2.304(5)
Fe-O		2.244(2)	2.193(4)
Fe-O(B)		1.7816(7)	1.7795(8)
Fe-Fe'		3.563(1)	3.559(1)
X-Fe-N(1)	X = Cl	102.18(9)	X = N(A) 102.1(2)
X-Fe-N(3)		105.3(1)	105.4(2)
X-Fe-N(5)		162.37(7)	161.5(2)
X-Fe-O		86.96(7)	85.7(2)
X-Fe-O(B)		104.01(3)	100.5(2)
N(1)-Fe-N(3)		150.8(1)	150.6(2)
N(1)-Fe-N(5)		74.8(1)	74.7(2)
N(1)-Fe-O		88.0(1)	86.3(2)
N(1)-Fe-O(B)		92.50(8)	93.0(1)
N(3)-Fe-N(5)		76.1(1)	75.9(2)
N(3)-Fe-O		83.8(1)	85.5(2)
N(3)-Fe-O(B)		90.34(8)	92.2(1)
N(5)-Fe-O		75.6(1)	76.0(2)
N(5)-Fe-O(B)		93.52(7)	97.8(1)
O-Fe-N(B)		168.62(7)	173.7(1)
O-Fe-O(B)-Fe'		180	180

* Primes denote atoms at positions $-x, -y, -z$.

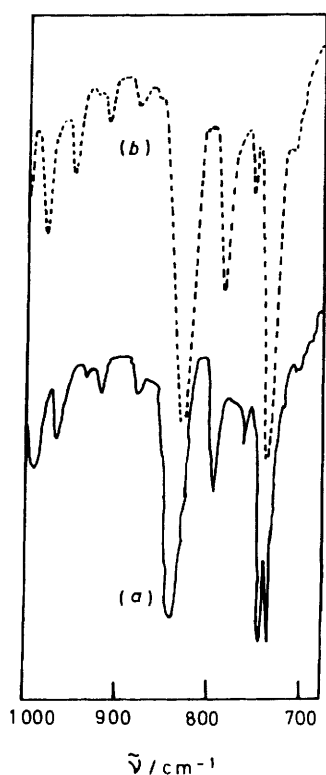


Figure 4. Infrared spectra of (a) $[\text{Fe}_2\text{O}(\text{bbimae})_2\text{Cl}_2][\text{NO}_3]_2$ (1) and (b) $[\text{Fe}_2\text{O}(\text{bbimae})_2(\text{NCS})_2][\text{NO}_3]_2$ (2)

benzimidazole molecules A and B' (cf. Figures 2 and 3) are almost parallel, and the dihedral angles are 7.1 and 9.8° for (1) and (2), respectively.

Table 5. Mössbauer data for compounds (1) and (2)

T/K	$\delta/\text{mm s}^{-1}$ *	
	(1)	(2)
78	0.51	0.57
295	0.40	0.40
	$ \Delta E_q /\text{mm s}^{-1}$	
	(1)	(2)
78	1.31	1.27
295	1.23	1.16

* Relative to metallic iron.

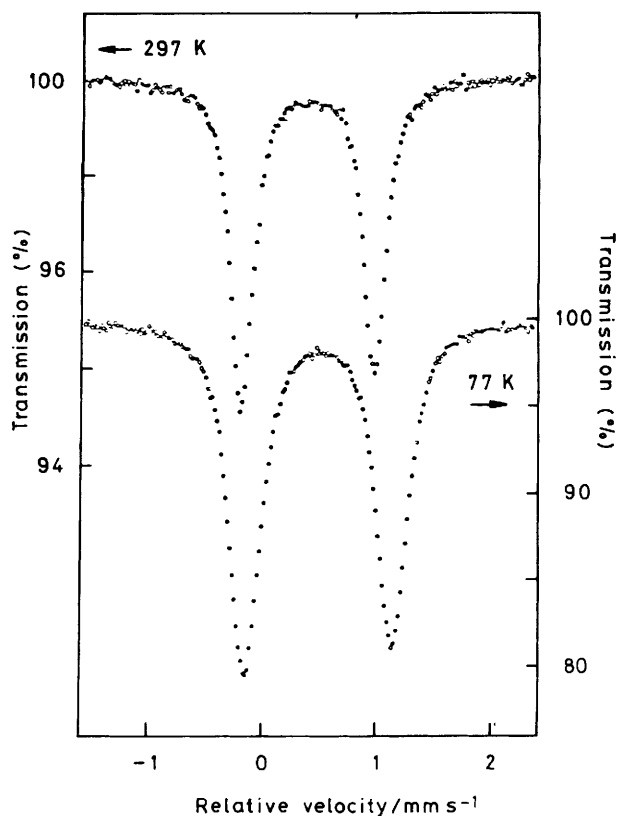


Figure 5. Mössbauer spectra of $[\text{Fe}_2\text{O}(\text{bbimae})_2(\text{NCS})_2][\text{NO}_3]_2$ (2)

Infrared Spectra.—The i.r. spectra of complexes (1) and (2) in the range 700–1 000 cm^{-1} are shown in Figure 4. Peaks at 841 and 833 cm^{-1} may be assigned to the antisymmetric stretch of Fe–O–Fe⁶ for (1) and (2), respectively, since such bands have not been observed in the spectra of other complexes of bbimae.^{11d}

Mössbauer Spectra.—The Mössbauer spectra at 77 and 297 K show an asymmetric quadrupole doublet, as illustrated by complex (2) in Figure 5. The isomer shifts (δ) and quadrupole splittings ($|\Delta E_q|$) are summarized in Table 5. These values were obtained by the least-squares fit of the experimental points assuming Lorentzian absorption lines. Since the isomer shifts for high-spin mononuclear and μ -oxo-bridged binuclear iron(III) complexes generally fall in the range 0.3–0.6 mm s^{-1} (relative to metallic iron),^{6,21} the present data (cf. Table 5) are also consistent with the presence of high-spin iron(III) ions in (1) and (2).

Table 6. Magnetic and structural data for oxo-bridged binuclear Fe^{III} complexes

	Fe–O–Fe/ ^o	Fe–O/Å	Fe–Fe/Å	–J/cm ^{–1}	Ref.
[Fe ₂ O(bbimae) ₂ Cl ₂][NO ₃] ₂	180	1.782	3.563	103	This work
{[Fe(cpydca)(H ₂ O) ₂] ₂ O}	180	1.773	3.545	107	8
[Fe(salen)] ₂ O ^b	142	1.791	3.40	95	c
		1.797			
[Fe(Hedta)] ₂ O ^{2–d}	165	1.79	3.56	99	e
		1.78			
		1.774			
[Fe(por)] ₂ O ^e	161	1.774	3.525	107.5	7
		1.800			
		1.787			
[Fe ₂ O(phen) ₄ (H ₂ O) ₂][NO ₃] ₄	155	1.787	3.49	110	9
		1.783			

^a H₂cpydca = 4-chloropyridine-2,6-dicarboxylic acid. ^b H₂salen = NN'-ethylenebis(salicylideneimine). ^c P. Coggon, A. T. McPhail, P. M. Groves, F. E. Mabbs, and V. N. McLachlan, *J. Chem. Soc. A*, 1971, 1014. ^d H₄edta = ethylenediaminetetra-acetic acid. ^e S. J. Lippard, H. Schugar, and C. Walling, *Inorg. Chem.*, 1967, **6**, 1825. ^f H₂por = porphyrin.

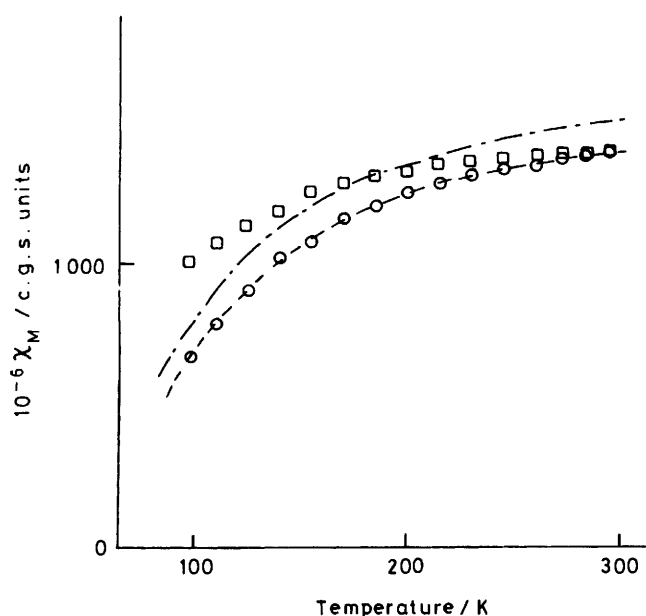


Figure 6. Variation with temperature of the molar susceptibility (per Fe³⁺) of [Fe₂O(bbimae)₂Cl₂][NO₃]₂ (1) (○) and [Fe₂O(bbimae)₂(NCS)₂][NO₃]₂ (2) (□). Values calculated from equation (1) are (---) with $g = 2.0$, $J = -102.8 \text{ cm}^{-1}$, $N\alpha = 0$, and (— · — · —) with $g = 2.0$, $J = -96 \text{ cm}^{-1}$, $N\alpha = 0$

Magnetic Properties.—Plots of molar susceptibility *vs.* temperature for (1) and (2) are shown in Figure 6. The magnetic moments of 1.81 (295 K) and 0.73 (98 K) B.M. for (1), and 1.82 (295 K) and 0.89 B.M. (98 K) for (2), indicate the operation of a moderate antiferromagnetic interaction between the two high-spin iron(III) ions. The expression for the temperature-dependent magnetic susceptibility derived from the general isotropic exchange Hamiltonian ($\mathcal{H} = -2JS_1 \cdot S_2$ for $S_1 = S_2 = \frac{5}{2}$) is given by⁶ equation (1). Based on the experimental

$$\chi = N\beta^2 g^2 \left[\frac{\exp(2J/kT) + 5\exp(6J/kT) + 14\exp(12J/kT) + 30\exp(20J/kT) + 55\exp(30J/kT)}{kT[1 + 3\exp(2J/kT) + 5\exp(6J/kT) + 7\exp(12J/kT) + 9\exp(20J/kT) + 11\exp(30J/kT)]} \right] + N\alpha \quad (1)$$

values (98–295 K), J was evaluated by the least-squares method to be -103 cm^{-1} for (1) with $g = 2.0$ and $N\alpha = 0$. Although the fitting was not satisfactory for (2), $-J$ was roughly

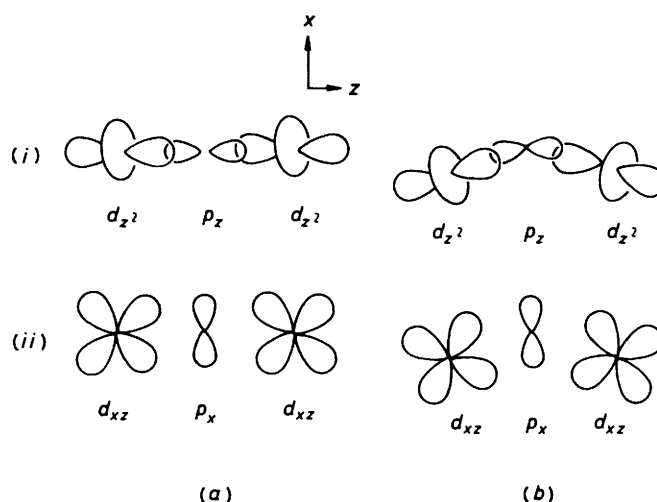


Figure 7. Overlap between iron 3*d* and oxygen 2*p* orbitals in linear (a) and bent (b) Fe–O–Fe systems for σ (i) and π (ii) pathways. The Fe–O distances are constant. The x axis is in the Fe–O–Fe plane

estimated to fall within the range 95–105 cm^{-1} on the basis of the magnetic moment at room temperature.

Magnetic Interaction and Structure.—In Table 6, the structural and magnetic properties of oxo-bridged binuclear iron(III) complexes are summarized. These data suggest that J is not sensitive to the Fe–O–Fe bond angle.

Since the Fe–Fe distances are in the range 3.4–3.6 Å, the contribution from direct metal–metal overlap to the spin-exchange mechanism must be small. Spin exchange must occur *via* superexchange pathways. In the d^5 – d^5 system, the σ - and π -superexchange pathways can be operative, and are illustrated in Figure 7. In the case of a bent Fe–O–Fe system, the contribution from the σ -pathway decreases relative to that in the linear Fe–O–Fe system, because of the decreasing overlap between the p_z orbital of the oxygen atom and d_{z^2} orbitals of the iron(III) atoms, as shown in Figure 7. On the other hand, the contribution from the π -pathway may be enhanced by increasing the overlap between the oxygen p_x and iron d_{xz} orbitals when the Fe–O–Fe angle is reduced from 180°. Thus in total, the magnetic interaction in oxo-bridged binuclear iron(III) complexes is not very sensitive to the Fe–O–Fe bond angle if the Fe–O bond distances are kept constant.

References

- 1 W. P. Griffith, *Coord. Chem. Rev.*, 1970, **5**, 45.
- 2 T. G. Spiro and P. Saltman, *Struct. Bonding (Berlin)*, 1969, **6**, 116.
- 3 H. B. Gray, *Adv. Chem. Ser.*, 1971, **100**, 365.
- 4 A. K. Shiemke, T. M. Loehr, and J. S. Loehr, *J. Am. Chem. Soc.*, 1984, **106**, 4951.
- 5 B. M. Sjoberg, T. M. Loehr, and J. S. Loehr, *Biochemistry*, 1982, **21**, 96.
- 6 K. S. Murray, *Coord. Chem. Rev.*, 1974, **12**, 1; H. B. Gray and H. J. Schugar, 'Inorganic Biochemistry,' ed. G. Eichorn, Elsevier, New York, 1973, ch. 3.
- 7 J. T. Landrum, D. Grimmett, K. J. Halber, W. R. Scheide, and C. A. Reed, *J. Am. Chem. Soc.*, 1981, **103**, 2640.
- 8 C. C. Ou, R. G. Wollmann, D. N. Hendrickson, J. A. Potenza, and H. Schugar, *J. Am. Chem. Soc.*, 1978, **100**, 4717.
- 9 J. E. Plowman, T. M. Loehr, C. K. Schauer, and O. P. Anderson, *Inorg. Chem.*, 1984, **23**, 3553.
- 10 Y. Nishida, N. Oishi, and S. Kida, *Inorg. Chim. Acta*, 1980, **44**, L257; Y. Nishida, K. Takahashi, H. Kuramoto, and S. Kida, *ibid.*, 1981, **53**, L103; Y. Nishida, K. Takahashi, and S. Kida, *Mem. Fac. Sci. Kyushu Univ., Ser. C*, 1982, **13(2)**, 335; Y. Nishida, H. Shimo, and S. Kida, *J. Chem. Soc., Chem. Commun.*, 1984, 1611; Y. Nishida, M. Takeuchi, N. Oishi, and S. Kida, *Inorg. Chim. Acta*, 1985, **96**, 81; Y. Nishida, M. Takeuchi, H. Shimo, and S. Kida, *ibid.*, p. 115.
- 11 (a) Y. Nishida, K. Takahashi, and S. Kida, *Mem. Fac. Sci. Kyushu Univ., Ser. C*, 1981, **13(1)**, 27; (b) K. Takahashi, E. Ogawa, N. Oishi, Y. Nishida, and S. Kida, *Inorg. Chim. Acta*, 1982, **66**, 97; (c) K. Takahashi, Y. Nishida, and S. Kida, *ibid.*, 1983, **77**, L185; (d) K. Takahashi, Y. Nishida, and S. Kida, *Bull. Chem. Soc. Jpn.*, 1984, **57**, 2628.
- 12 Y. Nishida, H. Shimo, K. Takahashi, and S. Kida, *Mem. Fac. Sci. Kyushu Univ., Ser. C*, 1984, **14(2)**, 301.
- 13 N. F. Curtis, *J. Chem. Soc.*, 1961, 3147.
- 14 A. Earnshaw, 'Introduction to Magnetochemistry,' Academic Press, London, 1968.
- 15 H. Oshio, Y. Maeda, and T. Takashima, *Inorg. Chem.*, 1983, **22**, 2684.
- 16 P. Main, M. M. Woolfsen, and G. Germain, 'Computer Program for the Automatic Solution of Crystal Structure,' Universities of York (England) and Louvain (Belgium), 1971.
- 17 'International Tables for X-Ray Crystallography,' Kynoch Press, Birmingham, 1974, vol. 4.
- 18 R. F. Stewart, E. R. Davidson, and W. T. Simpson, *J. Chem. Phys.*, 1965, **42**, 3175.
- 19 S. Kawano, *Rep. Comp. Cent. Kyushu Univ.*, 1980, **13**, 39.
- 20 'Universal Crystallographic Computer Program System (UNICS),' ed. T. Sakurai, The Crystallographic Society of Japan, Tokyo, 1967.
- 21 W. H. Armstrong, A. Spool, G. C. Papaefthymiou, R. B. Frankel, and S. J. Lippard, *J. Am. Chem. Soc.*, 1984, **106**, 3653.

Received 31st December 1984; Paper 4/2160